Spectral Multiplexing for Scalable Quantum Photonics using an Atomic Frequency Comb Quantum Memory and Feed-Forward Control

Neil Sinclair,[1] Erhan Saglamyurek,[1] Hassan Mallahzadeh,[1] Joshua A. Slater,[1] Mathew George,[2,†] Raimund Ricken,[2] Morgan P. Hedges,[1,‡] Daniel Oblak,[1] Christoph Simon,[1] Wolfgang Sohler,[2] and Wolfgang Tittel[1,*]

[1]*Institute for Quantum Science and Technology, and Department of Physics & Astronomy, University of Calgary, 2500 University Drive NW, Calgary, Alberta T2 N 1N4, Canada*

[2]*Department of Physics - Applied Physics, University of Paderborn, Warburger Straße 100, 33095 Paderborn, Germany*

(Received 18 December 2013; published 29 July 2014)

Future multiphoton applications of quantum optics and quantum information science require quantum memories that simultaneously store many photon states, each encoded into a different optical mode, and enable one to select the mapping between any input and a specific retrieved mode during storage. Here we show, with the example of a quantum repeater, how to employ spectrally multiplexed states and memories with fixed storage times that allow such mapping between spectral modes. Furthermore, using a $Ti:Tm:LiNbO_3$ waveguide cooled to 3 K, a phase modulator, and a spectral filter, we demonstrate storage followed by the required feed-forward-controlled frequency manipulation with time-bin qubits encoded into up to 26 multiplexed spectral modes and 97% fidelity.

DOI: 10.1103/PhysRevLett.113.053603 42.50.Ex, 03.67.Hk, 32.80.Qk, 78.47.jf

Further advances towards scalable quantum optics [1,2] and quantum information processing [3,4] rely on joint measurements of multiple photons that encode quantum states (e.g., qubits) [3–5]. However, as photons generally arrive in a probabilistic fashion, either due to a probabilistic creation process or due to loss during transmission, such measurements are inherently inefficient. For instance, this leads to exponential scaling of the time required to establish entanglement, the very resource of quantum information processing, as a function of distance in a quantum relay [6]. This problem can be overcome by using quantum memories, which are generally realized through the reversible mapping of quantum states between light and matter [7,8]. For efficient operation, these memories must be able to simultaneously store many photon states, each encoded into a different optical mode, and subsequently (using feed forward) allow selecting the mapping between input and retrieved modes (e.g., different spectral or temporal modes). This enables making several photons arriving at a measurement device indistinguishable, thereby rendering joint measurements deterministic. For instance, revisiting the example of entanglement distribution, a quantum relay supplemented with quantum memories changes it to a repeater and, in principle, the scaling from exponential to polynomial [4,9].

Interestingly, for such multimode quantum memories to be useful, it is not necessary to map any input mode onto any retrieved (output) mode, but it often suffices if a single input mode, chosen once a photon is stored, can be mapped onto a specific output mode (e.g., characterized by the photon's spectrum and recall time) [4,10]. This ensures that the photons partaking in a joint measurement, each recalled from a different quantum memory, are indistinguishable, as required, e.g., for a Bell-state measurement. We emphasize that it does not matter if the device used to store quantum states also allows the mode mapping, or if the mode mapping is performed after recall using appended devices—we will refer to the system allowing storage and mode mapping as *the memory*.

To date, most research assumes photons arriving at different times at the memory (i.e., temporal multiplexing), and recall on demand in terms of variable storage time [7,8]. Here we show, with the example of a quantum repeater, that it is also possible to employ spectrally multiplexed states and storage devices with fixed storage times, supplemented with frequency shifts based on feed-forward control. Furthermore, we report measurements using a highly broadband solid-state memory [11] that demonstrate the required mapping between input and output modes with time-bin qubits encoded into up to 26 spectral modes and a fidelity of 0.97, thereby significantly violating the classical bound of $2/3$ [12].

It is worth noting that for applications requiring short storage times, such as in linear optics quantum computing, a low-loss fiber could be sufficient to delay photons until a feed-forward signal arrives. However, for applications such as a quantum repeater, in which storage times exceed around 10 μs, fiber transmission drops below 90% and hence quantum state storage based on light-matter interaction will be necessary. Additionally, light-matter interaction affords more flexibility to perform processing tasks other than delaying [13].

Much theoretical and experimental work aiming at the development of quantum memory has been reported over the past decade [7,8,14], and most criteria required for such a memory to be suitable for the aforementioned

 © 2014 American Physical Society

applications have been independently met. However, at most two (entangled) qubits have been stored simultaneously in a way that allowed selecting the mode mapping [15], and the scalability of the approach, which relied on encoding information into four spatial modes, to tens or hundreds of qubits and modes remains to be proven (we note related work by Lan *et al*. [16] that, however, is not based on memories as defined above).

Rare-earth-ion doped crystals cooled to cryogenic temperatures have demonstrated to be promising storage materials, and many benchmark results have been reported [11,17–22]. We emphasize that, when such crystals are used in conjunction with the atomic frequency comb (AFC) protocol, the independence of the multimode (i.e., multiphoton) capacity on optical depth constitutes an important advantage compared to other protocols [23]. However, choosing the time of recall using control lasers to perform the mode mapping in the storage device is challenging with an AFC memory [21,23].

Drawing from the well-known temporal multiplexing approach, Fig. 1 shows, with the example of a quantum repeater, how spectrally multimode quantum memories, including frequency shifters and filters, allow rendering photons indistinguishable without the need for a variable storage time. While a repeater that employs temporal multiplexing assumes all qubits to feature the same spectrum but to arrive at different times at the memory, our new approach assumes all qubits to arrive at the same time, but to feature distinct spectra (i.e., to be encoded into different frequency bins). The retrieval of a desired qubit at a given time and with a given spectrum can then be achieved by retrieving all qubits after the same storage time, selecting the shift of the spectra of all qubits such that the desired qubit occupies a previously agreed-upon frequency bin, and rejecting all other qubits using a filtering cavity. To quantify the performance of a quantum repeater based on spectral multiplexing, we calculate the average rate of successful distributions of entangled photon pairs over a lossy channel as a function of total distance. The results, shown in Fig. 2, show that useful performance can already be achieved with 100 spectral modes, which is clearly feasible in the near future. Further information regarding the derivation of these results, and comparison with the temporal multiplexing scheme are contained in the Supplemental Material [24].

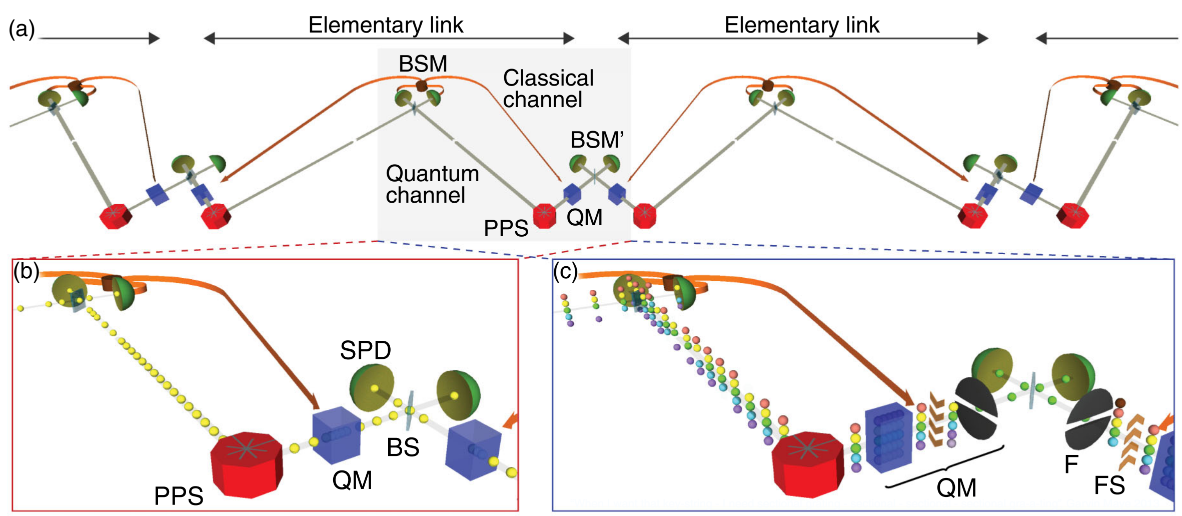

FIG. 1 (color online). Quantum repeater. (a) Block diagram of a section of a quantum repeater that does not employ qubit multiplexing. A source generating entangled pairs of photons (PPS) is located at the end point of each elementary link (i.e., node). One member per pair is stored in a quantum memory (QM), and the second member is sent over a “quantum channel” to the center of the link where it meets a member of an entangled pair generated at the other end of this link. The two photons’ joint state undergoes a Bell-state measurement (BSM)—comprised of a beam splitter (BS) and two single photon detectors (SPDs), and the result is communicated over a “classical channel” back to the end points to herald the establishment of entangled quantum memories by means of entanglement swapping [4,9,25]. Entanglement is stored until the two memories that are part of an adjacent link, are also entangled. Then, photons are recalled from neighboring memories and subjected to BSM’. This results in the establishment of entanglement across the two links, and, by continuing this procedure with other links, entanglement is established between the end points of the entire channel. (b) [(c)] Operation of a repeater node assuming temporal [spectral] multiplexing. Members of entangled photon pairs, each featuring the same spectrum [temporal profile and arrival time] but separated in time [frequency], are simultaneously stored in multimode quantum memories. A heralding (feed-forward) signal, derived from a successful BSM at the center of each elementary link indicates which of the stored photons is to be used for the remaining step of the protocol. The heralded photons are then recalled from adjacent memories such that they arrive indistinguishably at the BSM’. For temporal multiplexing, memories that allow adjusting the recall time as well as time-resolved detection are required, while for spectral multiplexing, the memories must incorporate adjustable frequency shifts (FS) and spectral filtering (F), and the BSM must distinguish different frequency bins.

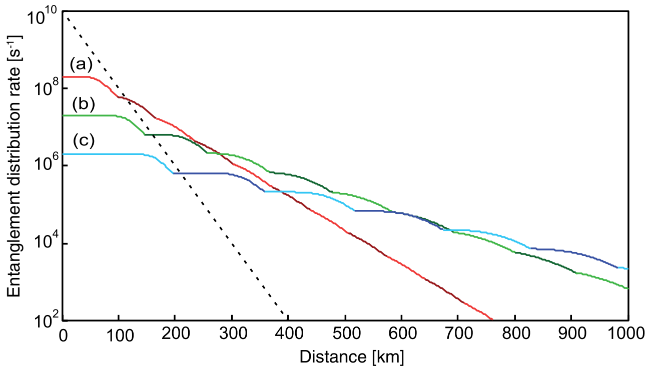

FIG. 2 (color online). Simulation of spectrally multiplexed quantum repeater performance. Optimal average entanglement distribution rate as a function of total distance. We assume loss of 0.2 dB/km, maximally entangled photon pairs emitted with 90% probability per attempt, quantum memories with 90% efficiency and total storage bandwidth of 300 GHz, and single-photon detectors with 90% efficiency and negligible dark counts. Bicolored curves—where a change in shading indicates the addition of an elementary link—represent (a) 10^2 (shown in red), (b) 10^3 (shown in green), and (c) 10^4 (shown in blue) spectral modes. The dotted line represents the direct transmission of members of entangled photon pairs produced at 10 GHz.

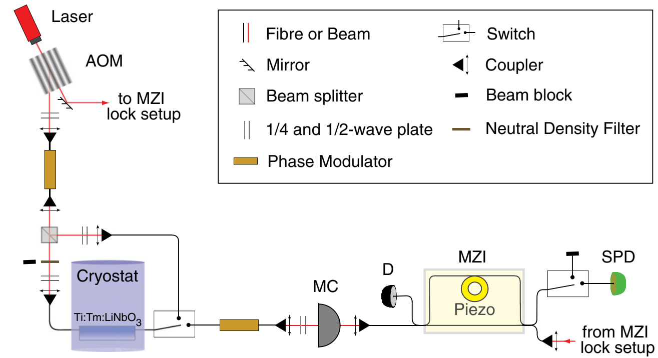

FIG. 3 (color online). Schematics of the experimental setup. The output of a frequency-stabilized continuous-wave laser at 795.4 nm wavelength is amplitude modulated with an AOM and serrodyne chirped [27] over disjoint frequency intervals using a phase modulator (PM). During 5 ms the laser light creates a broadband multimode AFC (see Fig. 4) in a Tm:Ti:$LiNbO_3$ waveguide located inside a 3 Kelvin cryostat and exposed to a magnetic field of 88 Gauss [11,26]. After a 2 ms wait time, during the next 5 ms, the AOM generates, with 4 MHz repetition rate, up to 26 spectrally multiplexed pairs of 15 ns-long Gaussian-shaped pulses (pulses in the pairs are separated by 20 ns), whose relative phases and central frequencies are set using the PM. The subsequent attenuator, or beam block, reduces the mean number of photons per pulse pair to 0.5, 0.1, or zero, respectively. The resulting time-bin qubits are then sent into the waveguide, and stored for 60 ns. Frequency-selective recall is achieved by means of a second PM, combined with a monolithic cavity (MC) having 70 MHz line width [28]. Finally, the recalled photons are detected using a Si-avalanche photodiode-based single photon detector (SPD) [allowing projections onto $|e\rangle$ and $|l\rangle$), or a phase-stabilized Mach-Zehnder interferometer (MZI) followed by a SPD (allowing projections onto $\frac{1}{\sqrt{2}}(|e\rangle \pm |l\rangle)$].

Conjecturing similarly promising results for other multiphoton applications, we now experimentally characterize the feasibility of multimode storage and feed-forward-controlled readout in the frequency domain. A schematic of our setup is depicted in Fig. 3. It performs four tasks: First, to prepare the memory, laser light is temporally and spectrally modulated, and then sent into a Ti:Tm:$LiNbO_3$ waveguide [11,26], thus spectrally tailoring the inhomogeneous absorption line of thulium into a series of equally spaced absorption peaks—an AFC. For multimode storage, the preparation procedure is repeated at different detunings with respect to the original laser frequency, resulting in twenty-six, 100 MHz-wide AFC's that are, with the exception of the region around zero detuning, spectrally separated by 200 MHz gaps (see Fig. 4). Second, our setup simultaneously generates many time-bin qubits of the form $|\psi\rangle = \alpha|e\rangle + \beta|l\rangle$, encoded into single-photon-level, phase randomized laser pulses of different intensities, in up to 26 frequency bins. Here, $|\alpha|^2 + |\beta|^2 = 1$, and $|e\rangle$ and $|l\rangle$ describe early or late emitted laser pulses, respectively. Third, the qubits are sent into the waveguide memory, where the absorption of each photon occupying a specific frequency bin leads to a collective excitation shared by the atoms forming the corresponding AFC. After a preset storage time $T_s = 1/\Delta$ (where Δ is the AFC peak spacing), the photons are emitted in their original state and spectral mode [23]. For selecting the recalled mode, the spectra of all simultaneously recalled photons are frequency shifted using another phase modulator [27], and all but the desired photons are rejected using a filter cavity with fixed resonance frequency [28]. Finally, projection measurements onto time-bin qubit states $|e\rangle$ or $|l\rangle$, or $(|e\rangle \pm |l\rangle)/\sqrt{2}$ are performed. As we describe in detail in the Supplemental Material [24], we postprocess the measured data to assess a key figure of merit—the lower bound on the storage fidelity $\mathcal{F}_L^{(1)}$—only from laser pulses containing exactly one photon. This procedure justifies the use of attenuated laser pulses instead of single photons to encode qubits for the purpose of our investigation. Further details about the AFC preparation, qubit generation, measurements and fidelity calculations, as well as current limitations resulting in a 1.5×10^{-4} overall memory efficiency are contained in the caption of Fig. 3 and the Supplemental Material [24].

In the first experiment we simultaneously store 26 qubits, alternating between $|e\rangle$ and $|l\rangle$, each prepared in one of the 26 spectral bins containing AFCs. All qubits are recalled after 60 ns, and subsequently frequency shifted and spectrally filtered. Figure 4 shows histograms of detections as a function of time for 30 different frequency shifts, for which the cavity filtering is expected to select the recall of at most one qubit. Our results indicate that, with little cross talk from the directly neighboring frequency bins, we can simultaneously store many qubits featuring disjoint spectra,

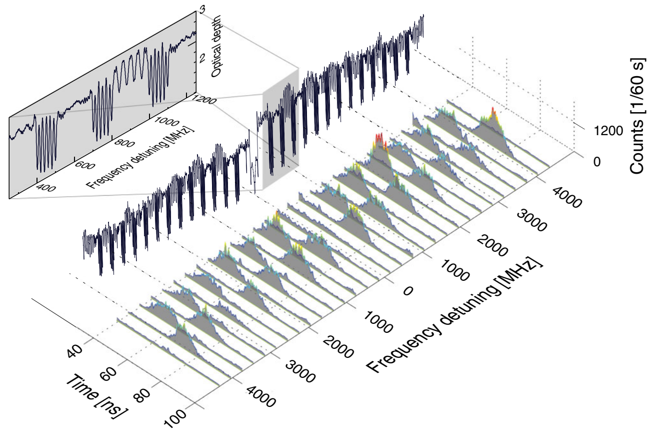

FIG. 4 (color online). Multimode storage and frequency selective recall. Histogram of arrival times of 26 simultaneously stored qubits, each containing 0.5 photons on average. Qubits are prepared in separate spectral modes and alternating temporal modes (i.e., $|e\rangle$ and $|l\rangle$), and are each recalled individually. The cavity resonance was set to 200 MHz detuning. No recall of qubits is observed in spectral modes at ± 150 and ± 4350 MHz detunings where no AFCs were prepared. The back panel and inset show the multibinned AFC absorption profile utilized. Modulation outside of the individual combs is due to higher order effects from the phase modulation.

and recall each qubit individually. We note that the total storage bandwidth of Tm:$LiNbO_3$ exceeds 300 GHz [29], which, in principle, allows expanding the current AFC to comprise more than 1000 spectral bins.

Next, to further examine the effect of cross talk between spectral modes, we first store and retrieve a "test" qubit prepared in $|l\rangle$ in the spectral bin having 1350 MHz detuning (with vacuum in all other spectral bins). We shift the test qubit into cavity resonance, and measure the probability to detect it in an early or a late temporal mode, which allows calculating the fidelity $\mathcal{F}_l$ of the recalled state with the input state (here and henceforth, the subscript index indicates the qubit's originally prepared state). We then increase the number of simultaneously stored qubits by creating them in neighboring spectral bins, and repeat the fidelity measurement with the test qubit. Note that all additional qubits are prepared in the orthogonal $|e\rangle$ state, such that the reduction of the fidelity of the test qubit due to cross talk is maximized. The result, further described in the Supplemental Material [24], shows that cross talk (due to the Lorentzian-shaped cavity resonance line) is restricted to qubits separated by at most two frequency bins.

Finally, we quantify the storage and recall fidelity for arbitrary qubit states stored in the AFC with multiple spectral bins shown in Fig. 4. Supported by the previous result, we create and simultaneously store time-bin qubits prepared in five spectral bins located between 750 and 1950 MHz detuning. A test qubit in state $|\psi\rangle \in [|e\rangle, |l\rangle, \frac{1}{\sqrt{2}}(|e\rangle + |l\rangle), \frac{1}{\sqrt{2}}(|e\rangle - |l\rangle)]$ is prepared in the central bin (at 1350 MHz detuning), and, for the reason already described above, the qubits in the four neighboring bins are prepared in the orthogonal state. We set the frequency shift to recall only the test qubit, and calculate the fidelity with its original state. This measurement is performed with mean photon numbers per qubit of 0.5, 0.1, and zero. Each measurement is taken over 60 s and the cavity resonance was set to a detuning of 3 GHz.

TABLE I. Storage and recall fidelities, $\mathcal{F}_{e/l}$ and $\mathcal{F}_{+/-}$, for test qubits encoded into attenuated pulses of mean photon number μ, and lower bounds $\mathcal{F}^{(1)}_{L,e/l}$ and $\mathcal{F}^{(1)}_{L,+/-}$ on storage and recall fidelities for qubits encoded into single-photon states ($n = 1$) derived using decoy state analysis [30]. One-standard-deviation uncertainties are calculated from statistical uncertainties of photon counts.

Photon input	$\mathcal{F}_{e/l}$	$\mathcal{F}_{+/-}$
$\mu = 0.5$	$(94.67 \pm 0.43)\%$	$(94.52 \pm 0.67)\%$
$\mu = 0.1$	$(91.56 \pm 1.35)\%$	$(85.14 \pm 2.73)\%$
$n = 1$	$(94.03 \pm 1.87)\%$	$(97.76 \pm 5.54)\%$

The resulting fidelities $\mathcal{F}_{e/l}$ and $\mathcal{F}_{+/-}$, averaged over each set of basis vectors [e.g., $\mathcal{F}_{e/l} = \frac{1}{2}(\mathcal{F}_e + \mathcal{F}_l)$], for mean photon numbers of 0.5 and 0.1 are displayed in Table I. In addition, the Table shows the lower bounds on the fidelities that we would have obtained if, with no other things changed, we had performed our experiments with qubits encoded into individual photons. These bounds, denoted by $\mathcal{F}^{(1)}_{L,e/l}$ and $\mathcal{F}^{(1)}_{L,+/-}$, are derived using a decoy state method that underpins the security of quantum key distribution based on attenuated laser pulses (a further explanation of this method is found in the Supplemental Material [24] and [30]). We find that all fidelities exceed the maximum value of 2/3 achievable using a classical memory [12]. Deviations from unity fidelity are due to the limited frequency shift efficiency of the phase modulator, limited suppression of the cavity, limited visibility and stability of the Mach-Zehnder interferometer used for certain projection measurements, and the remaining laser frequency and power fluctuations. Furthermore, the measurements with mean photon number of 0.1 are impacted by system loss and detector dark counts. Finally, by averaging the single-photon fidelities over all (properly weighted) input states, we derive our key figure of merit—the lower bound on the single-photon fidelity $\mathcal{F}^{(1)}_L = \frac{1}{3}\mathcal{F}^{(1)}_{L,e/l} + \frac{2}{3}\mathcal{F}^{(1)}_{L,+/-} = 0.97 \pm 0.04$. It exceeds the classical bound by 7.5 standard deviations, proving our memory to be suitable for applications of quantum optics and quantum information science.

In conclusion, we have shown for the first time that it is possible to combine the simultaneous storage of multiple qubits with feed-forward controlled mapping between input and output modes using a protocol that allows scaling the number of qubits to many hundreds. This is likely to accelerate the development of quantum repeaters, linear optics quantum computing, and advanced quantum optics experiments, in particular, if our frequency-based approach is combined with multiplexing using other degrees of freedom. For instance, considering as few as 10 frequency, 10 temporal, and 10 spatial modes, photons in 1000 different modes can be multiplexed, which already suffices for a quantum repeater. Or, considering 500 frequency, 10 spatial [16], and 400 temporal modes [31], one could simultaneously store 10^6 qubits. Note that any multiplexed degree of freedom can be manipulated to render photons indistinguishable—in our demonstration we used frequency.

This work is supported by Alberta Innovates Technology Futures (AITF), the National Sciences and Engineering Research Council of Canada (NSERC), the U.S. Defense Advanced Research Projects Agency (DARPA) Quiness Program under Grant No. W31P4Q-13-1-0004, the Killam Trusts, and the Carlsberg Foundation. The authors thank Thierry Chanelière for help with the laser locking system, Vladimir Kiselyov for technical support during various stages of the experiment, and Alex Lvovsky for lending us the filtering cavity.

[*]Corresponding author.
wtittel@ucalgary.ca
[†]Present address: Department of Physics, CMS College, Kottayam 686 001, India.
[‡]Present address: Department of Physics, Princeton University, Jadwin Hall, Princeton, New Jersey 08544, USA.

[1] Focus Issue: December 2009. Nat. Photonics **3**, 669 (2009).
[2] M. Scully and M. Zubairy, *Quantum Optics* (Cambridge University Press, Cambridge, England, 1997).
[3] P. Kok , W. J. Munro, K. Nemoto, T. C. Ralph, J. P. Dowling, and G. J. Milburn, Rev. Mod. Phys. **79**, 135 (2007).
[4] N. Sangouard, C. Simon, H. de Riedmatten, and N. Gisin, Rev. Mod. Phys. **83**, 33 (2011).
[5] J. Nunn, N. K. Langford, W. S. Kolthammer, T. F. M. Champion, M. R. Sprague, P. S. Michelberger, X.-M. Jin, D. G. England, and I. A. Walmsley, Phys. Rev. Lett. **110**, 133601 (2013).
[6] D. Collins, N. Gisin, and H. de Riedmatten, J. Mod. Opt. **52**, 735 (2005).
[7] A. I. Lvovsky, B. C. Sanders, and W. Tittel, Nat. Photonics **3**, 706 (2009).
[8] F. Bussières, N. Sangouard, M. Afzelius, H. de Riedmatten, C. Simon, and W. Tittel, J. Mod. Opt. **60**, 1519 (2013).
[9] H.-J. Briegel, W. Dür, J. I. Cirac, and P. Zoller, Phys. Rev. Lett. **81**, 5932 (1998).
[10] C. Simon, H. de Riedmatten, M. Afzelius, N. Sangouard, H. Zbinden, and N. Gisin, Phys. Rev. Lett. **98**, 190503 (2007).
[11] E. Saglamyurek, N. Sinclair, J. Jin, J. A. Slater, D. Oblak, F. Bussières, M. George, R. Ricken, W. Sohler, and W. Tittel, Nature (London) **469**, 512 (2011).
[12] S. Massar and S. Popescu, Phys. Rev. Lett. **74**, 1259 (1995).
[13] E. Saglamyurek, N. Sinclair, J. A. Slater, K. Heshami, D. Oblak, and W. Tittel, New J. Phys. **16**, 065019 (2014).
[14] C. Simon *et al.*, Eur. Phys. J. **58**, 1 (2010).
[15] H. N. Dai *et al.*, Phys. Rev. Lett. **108**, 210501 (2012).
[16] S.-Y. Lan, A. G. Radnaev, O. A. Collins, D. N. Matsukevich, T. A. B. Kennedy, and A. Kuzmich, Opt. Express **17**, 13639 (2009).
[17] C. Clausen, I. Usmani, F. Bussières, N. Sangouard, M. Afzelius, H. de Riedmatten, and N. Gisin, Nature (London) **469**, 508 (2011).
[18] M. P. Hedges, J. J. Longdell, Y. Li, and M. J. Sellars, Nature (London) **465**, 1052 (2010).
[19] I. Usmani, M. Afzelius, H. de Riedmatten, and N. Gisin, Nat. Commun. **1**, 12 (2010).
[20] M. Sabooni, Q. Li, S. Kröll, and L. Rippe, Phys. Rev. Lett. **110**, 133604 (2013).
[21] N. Timoney, I. Usmani, P. Jobez, M. Afzelius, and N. Gisin, Phys. Rev. A **88**, 022324 (2013).
[22] J. Jin, J. A. Slater, E. Saglamyurek, N. Sinclair, M. George, R. Ricken, D. Oblak, W. Sohler, and W. Tittel, Nat. Commun. **4**, 2386 (2013).
[23] M. Afzelius, C. Simon, H. de Riedmatten, and N. Gisin, Phys. Rev. A **79**, 052329 (2009).
[24] See Supplemental Material at http://link.aps.org/supplemental/10.1103/PhysRevLett.113.053603 for a detailed calculation of the proposed quantum repeater protocol, a short summary of the decoy state analysis, and details of the properties and performance of our spectral multimode quantum memory.
[25] C. H. Bennett, G. Brassard, C. Crépeau, R. Jozsa, A. Peres, and W. K. Wootters, Phys. Rev. Lett. **70**, 1895 (1993).
[26] N. Sinclair, E. Saglamyurek, M. George, R. Ricken, C. La Mela, W. Sohler, and W. Tittel, J. Lumin. **130**, 1586 (2010).
[27] L. M. Johnson, and C. H. Cox, J. Lightwave Technol. **6**, 109 (1988).
[28] P. Palittapongarnpim, A. MacRae, and A. I. Lvovsky, Rev. Sci. Instrum. **83**, 066101 (2012).
[29] Y. Sun, C. W. Thiel, and R. L. Cone, Phys. Rev. B **85**, 165106 (2012).
[30] X. Ma, B. Qi, Y. Zhao, and H.-K. Lo, Phys. Rev. A **72**, 012326 (2005).
[31] M. Bonarota, J. L. Le Gouët, and T. Chaneliere, New J. Phys. **13**, 013013 (2011).